Robotica (2009) volume 27, pp. 1–12. © 2008 Cambridge University Press
doi:10.1017/S026357470800444X Printed in the United Kingdom

Stable contour-following control of wheeled mobile robots

Juan Marcos Toibero, Flavio Roberti and Ricardo Carelli

Instituto de Automática – Universidad Nacional de San Juan, Av. San Martín Oeste 1109 – J5400ARL, San Juan, Argentina.
E-mail: {froberti, rcarelli}@inaut.unsj.edu.ar

(Received in Final Form: February 18, 2008. First published online: April 3, 2008)

SUMMARY

This paper presents a continuous wall-following controller for wheeled mobile robots based on odometry and distance information. The reference for this controller is the desired distance from the robot to the wall and allows the robot to follow straight wall contour as well as smoothly varying wall contours by including the curvature of the wall into the controller. The asymptotic stability of the control system is proved using a Lyapunov analysis. The controller is designed so as to avoid saturation of the angular velocity command to the robot. A novel switching scheme is also proposed that allows the robot to follow discontinuous contours allowing the robotic system to deal with typical problems of continuous wall-following controllers such as open corners and possible collisions. This strategy overcomes these instances by switching between dedicated behavior-based controllers. The stability of the switching control system is discussed by considering Lyapunov concepts. The proposed control systems are verified experimentally in laboratory and office environments to show the feasibility and good performance of the control algorithms.

KEYWORDS: Autonomous navigation, Switched systems, Mobile robots, Common Lyapunov function.

1. Introduction

Autonomous robots are robots which can perform desired tasks in unstructured environments without continuous human guidance. A way to deal with this problem is by decomposing it into individual *behaviors*,[1] such as move-to-goal, find-next-point, return-to-start, wander and halt. Then, these behaviors can be selected or fused according to a desired robot performance. A key feature for robot autonomy regards obstacle detection, identification and avoidance. In this context, a wall-following (WF) task is characterized by keeping a constant distance from the robot to a wall (or to an object) and can be properly combined with other tasks in order to obtain higher degrees of autonomy for the mobile platform, e.g., the skill *Go to goal avoiding obstacles* in ref. [2] Typically a WF controller has to recognize both distance and orientation errors between robot and wall. These two control states can be measured or estimated using, e.g., sonar,[2–10] laser rangefinder[11,13,21] or even with a force sensor that measures the robot-wall contact force.[19] Besides, WF controllers can be easily adapted for navigation along corridors by setting a desired distance relative to the centre of the corridor. Most WF controllers are path followers, because the focus is on controlling robot angular velocity while de translational velocity is kept constant.[3,7,10] Regarding sensors and robot/wall interaction, in spite the novelty in the approach,[19] the robot always needs a mechanical contact with the wall and seems like the robot is not able to deal with abrupt changes on the wall contour at the opposite side with respect to the force sensor.

It seems that that fuzzy-logic[3–5] or switching controllers[6–8] are the trend to deal with WF tasks. In an earlier work[9] a WF controller was used to avoid obstacles and to follow unknown walls. Then, ref. [5] proposes a way to extend the capabilities of this behavior but as a path planning problem, without describing the controller. In ref. [3] the contour following problem is treated by using a fuzzy logic controller. Here, the stability of the controller is not considered and the experimental results show difficulties in keeping a constant distance to the wall. More recently, E. Bicho[10] has used neural networks in order to estimate the relative robot/wall orientation, though the controller is not described through an explicit control law. A good contribution in switching control has been presented in ref. [8]. Here, a complete switching controller is proposed that allows the robot to track sharp discontinuous trajectories. This switching approach includes a formal stability demonstration at the switching times. However, the path to be tracked has to be previously known (discarding uncertainness on the environment around the robot) and the paper does not consider obstacle avoidance while tracking the trajectory. Therefore, this approach is a good option for map-based systems, but its applicability to reactive navigation in unknown environments is restricted.

Regarding the interaction between the robot and its surrounding environment, a WF controller becomes a useful means for reactive navigation in unknown environments. Actually, it can be used as an obstacle avoider by considering the obstacle as part of a wall to be followed.[3] Consequently, its capability to follow walls with several kinds of contours appears as a relevant issue that should be considered into the controller design; because this will allow the robot to avoid an ample range of obstacles. The inclusion of this new topic leads to a new control problem, namely, to deal with non-smooth wall contours (the contour-following problem.)

This paper addresses the problem of following the contour of unknown objects with unicycle-like mobile robots. The

* Corresponding author. E-mail: mtoibero@inaut.unsj.edu.ar

https://doi.org/10.1017/S026357470800444X Published online by Cambridge University Press

robot starts from an initial posture and must keep its distance to the object at a desired constant value. This WF problem is considered in a reactive fashion instead of the path planning approaches in refs. [6, 8, 20–21]; which in most cases need knowledge about the path to travel or an environment map/model. On the other hand, reactive strategies have a faster response time and require less computational costs in presence of uncertainness. This way, the complexity of the task to fulfill is often relaxed. Fore this work's goals, distance information (a laser rangefinder) and odometry information in fully unknown environments are known.

The main contribution of this paper is the proposal of a novel behavior-based control system to solve the CF problem. The proposed control system switches among three different controllers, each one designed to solve a specific instance of the navigating task: re-orientation (to avoid collisions), wall-following (for walls with nearly constant contour) and circle-performer (to recover the wall information in open corners.) The switching logic depends on sensor information about the fully unknown robot environment. Unlike most papers found in the literature dealing with WF or CF,[3–7,10–11] this work includes stability analysis for each individual behavior controller, and at switching times[15–17] for the overall switching system. Additionally, several experimental results are presented for illustrating the good performance of this control system and to show how the switching among three simple controllers allows the robot to achieve control objectives that would require a very complex conventional continuous controller. Other topics considered on this paper are the signal conditioning for the laser data, where a decentralized Kalman filter was considered to obtain more reliable values for the control states, and the saturation analysis for the robot angular velocity.

Possible applications for this strategy can be found in several areas. The most common is its use as an obstacle avoider in *move-to-goal* behaviors.[18] Other applications of a CF controller are the mapping of interior environments[6,11,21] in surveillance tasks[20] and within teleoperation contexts[4] using a similar behavior for telecommanding a mobile robot as proposed in ref. [22].

The paper is organized as follows. Section 2 presents the unicycle-like mobile robot kinematics. Section 3 proposes a WF saturation-free controller[13] to maintain a desired robot-to-wall distance for straight and smooth varying walls. Next, Section 4 presents a switching scheme that increases the robot skills allowing the robot to follow non-smooth varying walls. Finally, in Section 5 several experimental results are shown in order to state the performance of the controllers.

2. Mobile Robot

The unicycle-type wheeled mobile robot is considered in this paper. Before describing the robotic model composed by the robot kinematics, let us set the notation. With reference to Fig. 1, the global or task coordinate system is denoted by [W] and the coordinate system attached to the robot by [R]. The robot state variables are x, y and θ; where x, y are the coordinates of the middle point between the driving wheels and θ denotes the heading of the vehicle relative to the ^{W}X-axis of the world coordinate system. The vector $[\,x\ y\ \theta\,]^T$

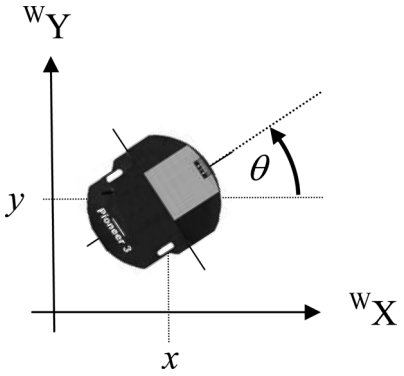

Fig. 1. Unicycle mobile robot world and robot coordinate systems.

defines the posture of the vehicle. A rear wheel turns freely and balances the rear end of the robot above the ground. The kinematics of the robot can be modeled by the equation

$$\begin{bmatrix} \dot{x} \\ \dot{y} \\ \dot{\theta} \end{bmatrix} = \begin{bmatrix} \cos(\theta) & 0 \\ \sin(\theta) & 0 \\ 0 & 1 \end{bmatrix} \begin{bmatrix} v \\ \omega \end{bmatrix} \tag{1}$$

where v and ω are the control inputs, i.e., the linear and the angular velocity, respectively. It is assumed a non-slip condition on the wheels, so the robot cannot move sideways. This is the nonholonomic constraint of the unicycle robot.

The robot is equipped with a laser radar sensor. As it can be seen in Fig. 2, the lateral beams from 0° to 15° (and from 165° to 180°) are used to estimate the object contour angle, and all of the beams are used to define a *guard-zone or safety-zone*, the purpose is to detect possible collisions between the robot and the object. This rectangular guard-zone is defined by two parameters: the desired lateral (d_{lat}) and frontal (d_{front}) distance. The minimum lateral value for a Pioneer IIIDX is about 330 mm.

The selection of the side of the object to follow is based on the initial conditions. Firstly the robot computes the object orientation and the distance to the object for its right side and also for its left side. Then, the robot will take the nearest side to follow and will keep following this side.

Each beam is identified by its angle. For example, for the beam at 0°, the notation d_{000} is used to denote the distance measured by this beam. Without loosing generality and to simplify the notation, it will be assumed that the robot follows only the wall at the right side of the robot.

3. Wall-Following Controller (Straight and Smooth Varying Walls)

3.1. Wall angle computation

The wall angle θ_{wall} estimation with respect to the world coordinate system is performed using only two beams: one perpendicular to the heading of the robot d_{000}, and the other may be selected depending on the desired robot-wall distance. In order to obtain a more reliable value, this paper considers a group of ten beams at each side of the robot, thus resulting ten different angle values. These values are

https://doi.org/10.1017/S026357470800444X Published online by Cambridge University Press

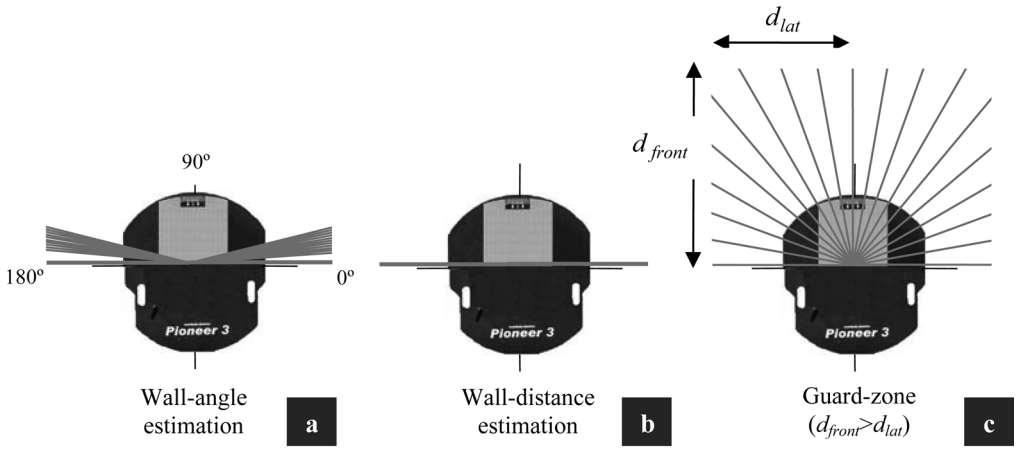

Fig.2 Laser radar

Fig. 2. Laser radar.

then fused together using a decentralized Kalman filter[12] which gives an improved estimation for the wall angle θ_{wall}. Estimation is performed by considering the following steps:

i) Distances to the wall are obtained by each laser beam; these measures denoted as d_{010} for a 10° angle, d_{011} for a 11° angle and so on;
ii) With the distance and the current position of the robot, the end-point of each beam is computed, e.g. for the laser beam at 10°, according to

$$x_{010} = x + d_{010}\,\cos(\theta - 80^\circ) \tag{2a}$$

$$y_{010} = y + d_{010}\,\sin(\theta - 80^\circ) \tag{2b}$$

iii) The wall angle can be now easily calculated

$$\theta^{010}_{\text{wall}} = \tan^{-1}\left(\frac{-\Delta y}{-\Delta x}\right) = \tan^{-1}\left(\frac{y_{010} - y_{000}}{x_{010} - x_{000}}\right) \tag{3}$$

where the superscript specifies the angle used for the computation. From (3) it is assumed a linear connection between both points. Figure 3 shows an example of this estimation.
iv) Finally, ten different estimations for the angles between 6° and 15° degrees are fused together thus obtaining a single value for wall angle.

This section aims at obtaining the optimal value θ_{wall} for wall angle. To do this, ten sequences of measures θ^i_{wall} (with $i = 6, 7, \ldots, 15$) are available in correspondence with the ten laser beams employed. Next, two separate stages are considered; first, a Kalman filter is used for each sequence in order to obtain the optimal value for the ith sequence: $\theta^{iOPT}_{\text{wall}}$; second, another master Kalman filter is used to obtain the final value for θ_{wall} resulting from the fusion of the previous $\theta^{iOPT}_{\text{wall}}$ values. So, for the ith sequence, it is assumed that

$$\theta^i_{\text{wall}} = \theta^{iOPT}_{\text{wall}} + v^i \tag{4}$$

where v^i is a zero mean random variable with covariance R^i. The block diagram of Fig. 4 shows the local filters (one for each measurement sequence), the master filter as well as the different involved variables.

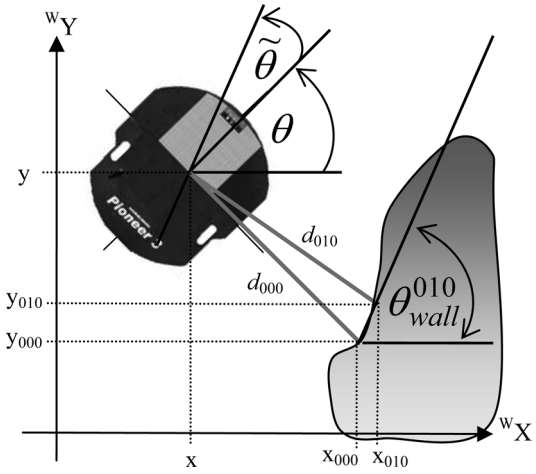

Fig. 3. Wall angle computation. resulting as a value $\theta^{010}_{\text{wall}}$ for the wall-angle related to robot posture x, y, and θ in the world coordinate system for the beam at 10°.

The mean and the covariance for each measuring sequence is computed recursively, according to

$$\hat{\theta}^i_{\text{wall}} = \hat{\theta}^i_{\text{wall}} + \mu\,\left(\theta^i_{\text{wall}} - \hat{\theta}^i_{\text{wall}}\right) \tag{5}$$

$$R^i = R^i + \mu\,\left(\left(\theta^i_{\text{wall}} - \hat{\theta}^i_{\text{wall}}\right)^2 - R^i\right) \tag{6}$$

where $\hat{\theta}^i_{\text{wall}}$ refers to the mean value of the sequence θ^i_{wall} and $0 < \mu < 1$ is a design constant. Note that the subscripts that denote time instants were omitted for clarity reasons. Next, each sequence is filtered individually:

$$(P^i)^{-1} = (M^i)^{-1} + (R^i)^{-1} \tag{7}$$

$$\theta^{i.OPT}_{\text{wall}} = P^i\left[m^i\,(M^i)^{-1} + (R^i)^{-1}\,\theta^i_{\text{wall}}\right]. \tag{8}$$

Equation (7) gives the information matrix update, while (8) states the estimate update; M^i and m^i are the error covariance and the prior estimation values for the measurement sequence θ^i_{wall}, respectively. All the filtered values are fused together

https://doi.org/10.1017/S026357470800444X Published online by Cambridge University Press

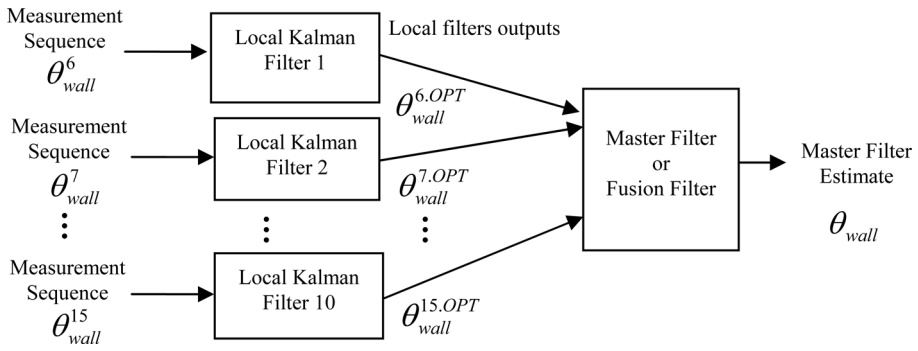

Fig. 4. Fusion block diagram.

to obtain the optimal value for the wall angle

$$\theta_{\text{wall}} = P\left[\frac{m}{M} + \sum_i \left(\frac{\theta^{i.OPT}_{\text{wall}}}{P^i} - \frac{m^i}{M^i}\right)\right] \tag{9}$$

with

$$P^{-1} = M^{-1} + \sum_i [(P^i)^{-1} - (M^i)^{-1}]. \tag{10}$$

The updates for each cycle of the loop are given by

$$M^i = P^i \tag{11a}$$
$$m^i = \theta^{i.OPT}_{\text{wall}} \tag{11b}$$
$$m = \theta_{\text{wall}} \tag{11c}$$
$$M = P. \tag{11d}$$

3.2. Robot-wall distance computation

The robot to wall distance computation considering a wall at the right side of the robot is obtained by

$$d_{\text{wall}} = d_{000}\cos(\tilde{\theta}) \tag{12}$$

where $\tilde{\theta}$ is the difference between the heading angle of the robot and the wall angle (Fig. 3). This angle will be properly defined in the next paragraphs. A similar expression for the distance to a wall at the left side of the robot can be obtained by replacing d_{000} for d_{180}. Note that, according to (12), this distance could not represent the actual robot-wall distance but it is a good approximation for control purposes.

3.3. Controller description and analysis

This controller renders a control law for wall-following based on laser sensorial information and odometry of the robot. The reference for this controller is the desired distance from the robot to the wall d_{des}. From Fig. 5, the control errors are defined as follows

$$\tilde{d} = d_{\text{des}} - d_{\text{wall}} \tag{13a}$$
$$\tilde{\theta} = \theta_{\text{wall}} - \theta \tag{13b}$$

Equation (13a) states the distance error between the actual distance to the wall and the desired distance to the wall d_{des} while (13b) states the orientation error between the estimated wall angle and the heading angle of the robot in the world coordinate system [W].

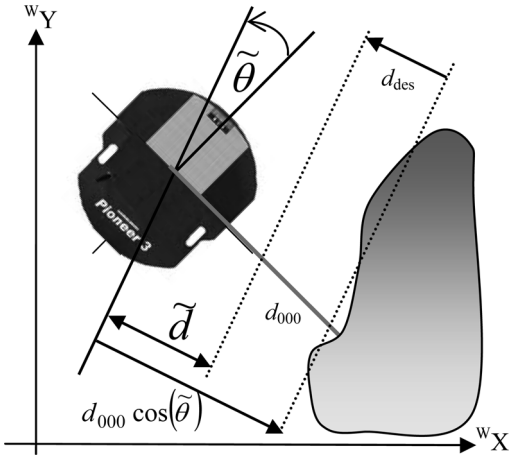

Fig. 5. Wall-following controller scheme. Distance error calculation. Note that the value for the distance error could be negative.

The time variations of the control errors are given by

$$\dot{\tilde{d}} = -v\,\sin(\tilde{\theta}) \tag{14a}$$
$$\dot{\tilde{\theta}} = \dot{\theta}_{\text{wall}} - \omega \tag{14b}$$

where, $\dot{\theta}_{\text{wall}}$ is the derivative of the reference for the wall orientation and is obtained from θ_{wall} by considering an Euler approximation. This derivative is null for straight wall. Now, taking into consideration the analysis of the control system, the following (globally positive definite and radially unbounded) Lyapunov candidate function is proposed.

$$V = \frac{1}{2}\tilde{\theta}^2 + \int_0^{\tilde{d}} k_{\tilde{d}}(\xi)\,\xi\,d\xi, \tag{15}$$

where function $k_{\tilde{d}}(\tilde{d})$ was selected as in ref. [14] in order to avoid actuator's saturation, and ξ is a dumb variable.

$$k_{\tilde{d}}(\tilde{d}) = \frac{k_1}{1 + |\tilde{d}|} \geq 0 \tag{16}$$

https://doi.org/10.1017/S026357470800444X Published online by Cambridge University Press

from here on, $k_{\tilde{d}}(\tilde{d})$ will be written as $k_{\tilde{d}}$ to simplify notation. The time derivative of the Lyapunov candidate function is

$$\dot{V} = \tilde{\theta}\dot{\tilde{\theta}} + k_{\tilde{d}}\tilde{d}\dot{\tilde{d}} \tag{17}$$

$$\dot{V} = \tilde{\theta}\,(\dot{\theta}_{\text{wall}} - \omega) - k_{\tilde{d}}\tilde{d}v\,\sin(\tilde{\theta}). \tag{18}$$

Then, the proposed control actions are

$$v = v_{\max} \geq 0 \tag{19a}$$

$$\omega = \dot{\theta}_{\text{wall}} + K_{\tilde{\theta}}\,\tanh\,(k_{\tilde{\theta}}\tilde{\theta}) - k_{\tilde{d}}\tilde{d}v\frac{\sin(\tilde{\theta})}{\tilde{\theta}}, \tag{19b}$$

where $v_{\max}$ is the desired linear velocity and $K_{\tilde{\theta}} \geq 0$ is a positive definite design constant, and $k_{\tilde{\theta}} > 0$ is a design constant that sets the maximum value and slope of the tanh function. As in (16), this inclusion is aimed at handling actuator saturation. The purpose of these functions will be explained in detail in Section 3.4.

By substituting (19) into (18), the derivative of the Lyapunov candidate function becomes

$$\dot{V} = -K_{\tilde{\theta}}\,\tilde{\theta}\,\tanh\,(k_{\tilde{\theta}}\tilde{\theta}) \leq 0. \tag{20}$$

Equation (20) states that the control system is Lyapunov stable but not asymptotically stable. To prove the asymptotic stability, the autonomous nature of the closed-loop system is considered. The closed-loop equations can be obtained by replacing the control actions into (14)

$$\dot{\tilde{d}} = -v_{\max}\,\sin(\tilde{\theta}) \tag{21a}$$

$$\dot{\tilde{\theta}} = -K_{\tilde{\theta}}\,\tilde{\theta}\,\tanh\,(k_{\tilde{\theta}}\tilde{\theta}) - k_{\tilde{d}}\tilde{d}v_{\max}\frac{\sin(\tilde{\theta})}{\tilde{\theta}}. \tag{21b}$$

By applying the Krasovskii-LaSalle theorem[23] in the region Ω, with

$$\Omega = \left\{\begin{bmatrix}\tilde{d}\\ \tilde{\theta}\end{bmatrix} : \dot{V}(\tilde{d},\tilde{\theta}) = 0\right\} \Rightarrow \left\{\begin{bmatrix}\tilde{d}\\ \tilde{\theta}\end{bmatrix} = \begin{bmatrix}\tilde{d}\\ 0\end{bmatrix}\right\} \tag{22}$$

the only invariant is $\tilde{d} = 0$. Therefore, by invoking the LaSalle's theorem, it can be concluded that the origin of the state space is globally uniformly asymptotically stable.

Remark. $\dot{\theta}_{\text{wall}}$ is included in order to cover, in stability analysis, the case of smoothly varying walls; but this controller can be considered with a null value for this derivative despite of a lower controller performance.

3.4. Saturation of the angular velocity

An important feature when designing controllers for mechanical systems is related to the saturation of control actions. It is desirable to obtain an expression for maximum values of control actions. The analysis of the saturation problem will be made by firstly considering the case of straight walls ($\dot{\theta}_{\text{wall}} = 0$) and, then, the case of smooth varying walls. Therefore, by considering a maximum value for the angular velocity: $\omega_{\max}$ in (19b), it is possible to obtain conditions for the design constants so as to avoid saturation of the control command. For straight walls this expression is

$$|\omega_{\max}| \geq \left| K_{\tilde{\theta}}\,\tanh\,(k_{\tilde{\theta}}\tilde{\theta}) + k_{\tilde{d}}\tilde{d}v_{\max}\,\frac{\sin(\tilde{\theta})}{\tilde{\theta}}\right|. \tag{23}$$

Then, substituting (16) into (23), and considering the saturation value $K_{\tilde{\theta}}$ in the first term and the maximum value of the second term at $\tilde{\theta} = 0$ and large $\tilde{d}$ values

$$|\omega_{\max}| \geq |K_{\tilde{\theta}} + k_1 v_{\max}|. \tag{24}$$

This latter expression allows selecting the design constants in such a way that $|\omega| < |\omega_{\max}|$. Now, when considering smooth varying walls an expression similar to (23) is now given by

$$|\omega_{\max}| \leq \left|\dot{\theta}_{\text{wall}} + K_{\tilde{\theta}}\,\tanh\,(k_{\tilde{\theta}}\tilde{\theta}) + k_{\tilde{d}}\tilde{d}v\frac{\sin(\tilde{\theta})}{\tilde{\theta}}\right|. \tag{25}$$

Then, substituting (16) into (25), and considering the saturation value $K_{\tilde{\theta}}$ in the second term and the maximum value of the third term at $\tilde{\theta} = 0$ and large $\tilde{d}$ values, a condition for $\dot{\theta}_{\text{wall}}$ is

$$|\dot{\theta}_{\text{wall}}| \leq |\omega_{\max}| - K_{\tilde{\theta}} - k_1 v_{\max}. \tag{26}$$

This expression gives a bound for the value $\dot{\theta}_{\text{wall}}$ (the time-variation of the wall-angle) that avoids saturation of the angular velocity for the maximum admissible value ω_{max}. That is, it gives the maximum value for the variation of the contour that will not produce an angular velocity larger than the prefixed value $\omega_{\max}$.

3.5. Note on the robot-wall relative position

It is important to mention that (14a) models the distance error variation for a wall at the right side of the robot. If the wall is placed on its left side, the expression to be considered changes to

$$\dot{\tilde{d}} = v\,\sin(\tilde{\theta}). \tag{27}$$

This changes the sign of (18) as well,

$$\dot{V} = \tilde{\theta}\,(\dot{\theta}_{\text{wall}} - \omega) + k_{\tilde{d}}\tilde{d}v\,\sin(\tilde{\theta}), \tag{28}$$

Finally, this sign must be compensated in the control action Eq. (19b)

$$\omega = \dot{\theta}_{\text{wall}} + K_{\tilde{\theta}}\,\tanh\,(k_{\tilde{\theta}}\tilde{\theta}) + k_{\tilde{d}}\tilde{d}v\,\frac{\sin(\tilde{\theta})}{\tilde{\theta}} \tag{29}$$

After these considerations the stability results are immediately extended for the new configuration.

3.6. Experimental results

The proposed control algorithm was proved in a real office setting with a Pioneer3-DX mobile robot. The robot length is about 330 mm. The values of the design parameters were set to: $k_1 = 0.025$, $K_{\tilde{\theta}} = 11.5$, $k_{\tilde{\theta}} = 0.3$ and $y_{\text{des}} = 500$ mm.

https://doi.org/10.1017/S026357470800444X Published online by Cambridge University Press

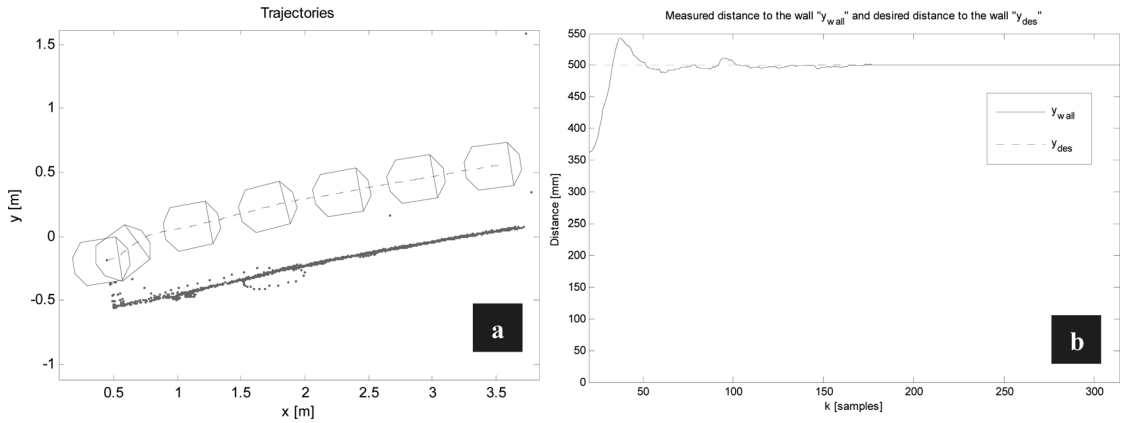

Fig. 6. (a) Trajectory described by the robot following a wall with straight contour. The contour of the wall was reconstructed by means of the laser information. (b) Distance between the robot and the straight wall. The linear velocity for this experiment was set to 200 mm/sec.

The selection for the values for k_1 and $K_{\tilde{\theta}}$ is based on the desired angular velocity saturation value according to (24) or (26) and on its influence on the controller performance: while k_1 corrects the distance error, $K_{\tilde{\theta}}$ corrects the robot-wall orientation error. A proper maximum value for linear velocity can be obtained by considering the robot inertia along with the length of the robot safety-zone (d_{front} in Fig. 2c).

In order to show the performance of the proposed controller, three different experiments were carried out. First, the robot follows a straight wall; second, it follows a wall with smoothly varying contour and finally, it follows an almost-circular contour.

From Figs. 6–8, the good performance of the proposed controller for wall-following can be concluded.[13] The error is less than 50 mm in all considered settings (a small value when compared to the size of the robot).

4. Contour-Following Controller

The WF controller proposed in Section 3 acting alone shows a good performance when following a wall, but there are two cases which it cannot deal with:

i) Abrupt variations in the contour of the object which makes it difficult to estimate the current object's angle. In this case (Fig. 9a), the distance measured by the laser beams varies suddenly.
ii) Abrupt variations in the contour due to an interior corner that causes the robot to crash against the object (Fig. 9b).

The first situation can be detected by computing the variance of the length of the lateral beams that estimates the wall angle. This variance has a value close to zero when the robot is following a wall, but it becomes large when the contour is lost. If the value of the variance is larger than a prefixed threshold value, then a *loss of wall* event is generated. In the second case, collisions are detected as an invasion of the safety-zone of the robot. If the length of any beam lies within the predefined safety-zone, then a *possible collision* event is generated. This work proposes to solve these problems by adding two new behaviors, one to deal with each situation, thus building a switching system.

4.1. Handling the case of missing the wall to follow

In this case, the robot has lost the wall to follow. This behavior is activated when non-consistent measurements of the control states $\tilde{\theta}$ and $\tilde{d}$ are obtained. The proposed solution is to describe a circular path of radius R on the floor (Fig. 10) until one of the following conditions is fulfilled:

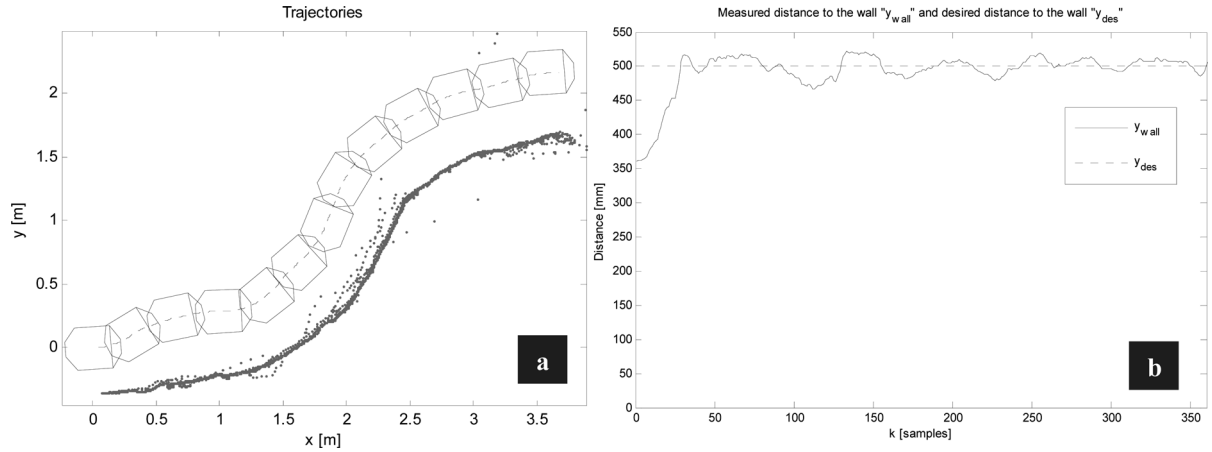

Fig. 7. (a) Trajectory described by the robot following a wall of variable contour. As it can be seen, the wall presents variations on its contour and on its texture. (b) Robot wall distance in the variable contour experiment.

https://doi.org/10.1017/S026357470800444X Published online by Cambridge University Press

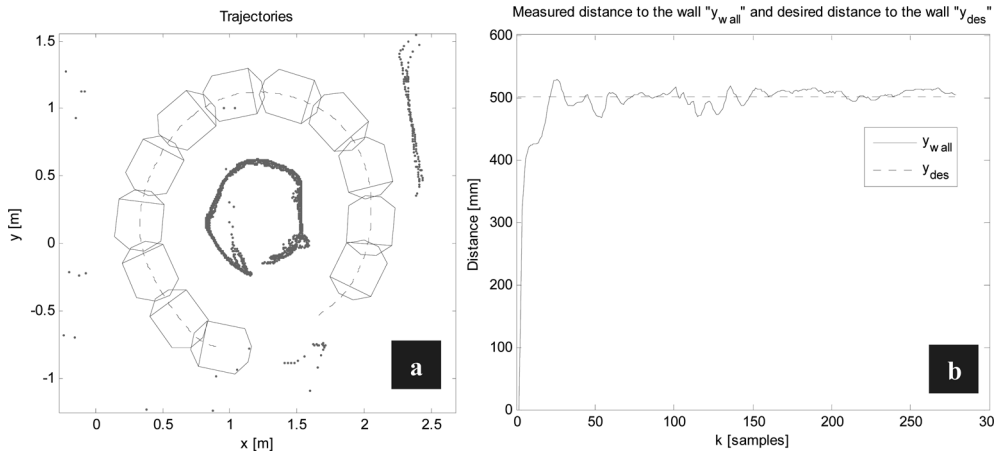

Fig. 8. (a) Robot following an almost-circular contour. The linear velocity for this experiment was set to 200 mm/s. (b) Robot wall distance in the circular path experiment.

i) The wall can be followed again using the wall-following behavior provided that $\tilde{d} = \tilde{d}_{\text{lost}}$ (Fig. 10(a) and Fig. 10(b)); being $\tilde{d}_{\text{lost}}$ the last value of $\tilde{d}$ just before switching. This way, it could be assumed that $\dot{\tilde{d}} = 0$ considering the value of $\tilde{d}$ does not change at the beginning and at the end of this behavior.
ii) A possible collision between the robot and the wall is detected (Fig. 10c), as considered in Section 4.2.

In the following instance, it is proposed a simple controller to describe a circular path of radius $R > 0$, based on the previous wall-following controller, though the distance error is not considered. Therefore, considering the following errors as in (13)

$$\tilde{\theta} = \theta_{\text{circ}} - \theta \tag{30}$$

where θ_{circ} is the heading reference to perform the desired circular path

$$\theta_{\text{circ}} = \pm \frac{v_{\max}}{R} t. \tag{31}$$

Here, the plus/minus sign of (31) denotes that the reference θ_{circ} will generate a left or right turn. That is, the robot will turn left (right) if it is following an object at its left (right) side. Then, replacing (31) into (30) and considering its time derivative

$$\dot{\tilde{\theta}} = \dot{\theta}_{\text{circ}} - \omega = \pm \frac{v_{\max}}{R} - \omega. \tag{32}$$

In order to analyze the stability of this control system, consider the following Lyapunov candidate function and its time derivative

$$V_{\tilde{\theta}} = \frac{\tilde{\theta}^2}{2} \tag{33}$$

$$\dot{V}_{\tilde{\theta}} = \tilde{\theta}\,\dot{\tilde{\theta}} = \tilde{\theta}\,(\dot{\theta}_{\text{circ}} - \omega) = \tilde{\theta}\left(\pm \frac{v_{\max}}{R} - \omega\right). \tag{34}$$

Now, to achieve the control objective, the following control actions are proposed

$$v = v_{\max} \tag{35a}$$

$$\omega = \pm \frac{v_{\max}}{R} + K_{\tilde{\theta}} \tanh(k_{\tilde{\theta}}\,\tilde{\theta}); \quad K_{\tilde{\theta}} > 0, k_{\tilde{\theta}} > 0. \tag{35b}$$

Finally, by replacing (35) in (34), the asymptotic stability of the control system can immediately be proved. That is, this

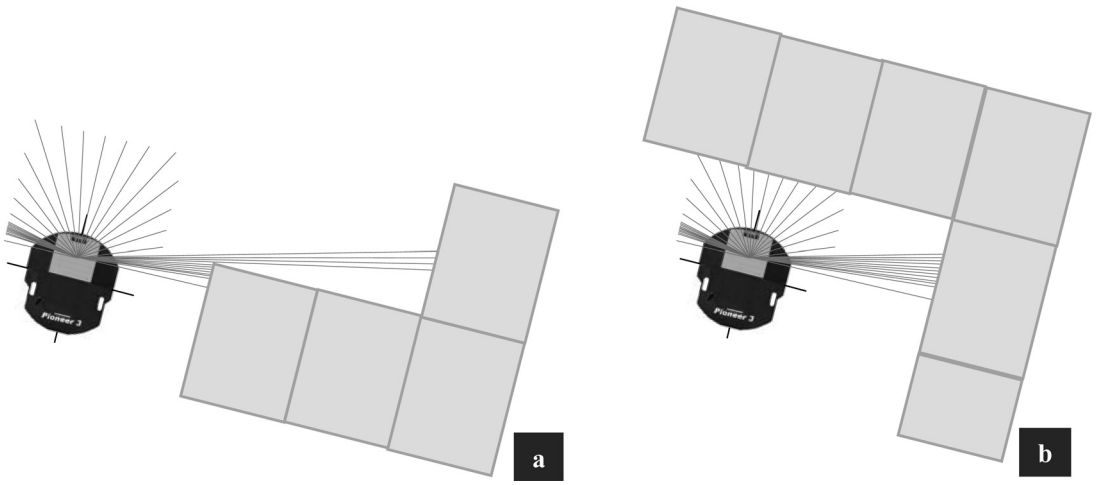

Fig. 9. Main problems when following contours: (a) the presence of an open corner and (b) the presence of an interior corner.

https://doi.org/10.1017/S026357470800444X Published online by Cambridge University Press

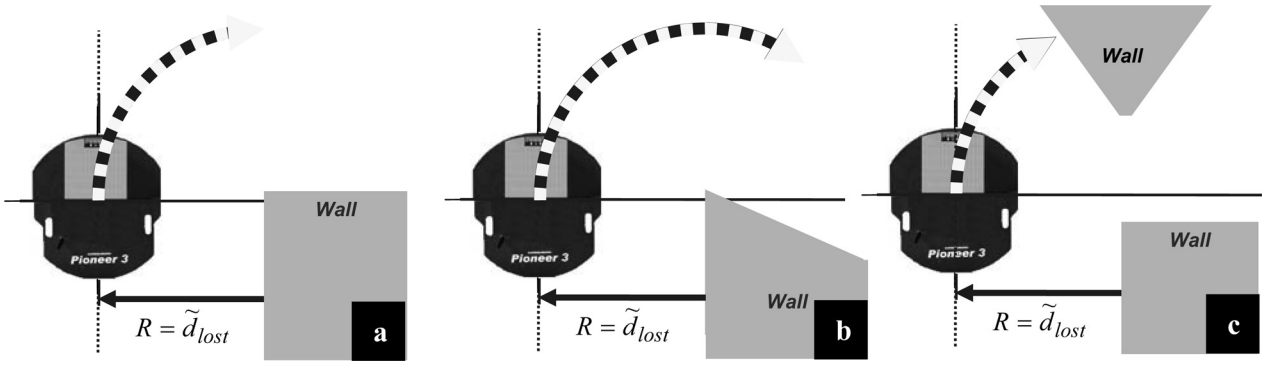

Fig. 10. Handling "*loss of wall*" situations.

controller guarantees that the robot will perform a circular path by acting only on the robot angular velocity.

4.2. *Handling possible collisions*

This behavior is activated when an obstacle appears in front of the robot at a distance $d_{\text{impact}} \leq d_{\text{front}}$, d_{impact} being the smallest distance to the obstacle measured inside the robot safety-area, which is also characterized by angle θ_{impact} on the laser range finder framework. Also, d_{front} (defined in Section 2) is selected to be equal to the actual robot wall distance d_{wall} and $d_{\text{lat}} < d_{\text{front}}$. The objective of this behavior is to avoid possible collisions by rotating the robot until a free-path condition (characterized by an empty safety-area) is again achieved, and $\tilde{d}_{k+T} = \tilde{d}_k$, where k is the obstacle detection instant, and T is the time during this behavior was active until switching to the wall-following behavior. Under the above mentioned conditions, this behavior will always achieve a free-path condition satisfying $\tilde{d}_{k+T} = \tilde{d}_k$ (see Fig. 11). Analogously to the behavior described in Section 4.1, it could be assumed that $\dot{\tilde{d}} = 0$, considering that $\tilde{d}$ does not change at the beginning and at the end of this behavior.

To this aim, the following controller that allows positioning the robot at a desired orientation angle θ_d is proposed. The orientation error between the heading angle of the robot and the desired orientation is defined as shown in Fig. 12

$$\tilde{\theta} = \theta_d - \theta, \tag{36}$$

where $\theta_d = \theta_{\text{impact}} \pm 90^\circ$ is a constant value that is updated so as to attain an open area.

Then, the time derivative of (36) is considered

$$\dot{\tilde{\theta}} = -\omega. \tag{37}$$

As regards the stability analysis of this controller, the Lyapunov candidate (33) is considered again, and the following control actions are proposed,

$$v = 0 \tag{38a}$$

$$\omega = K_{\tilde{\theta}} \tanh(k_\theta \tilde{\theta}); \quad K_{\tilde{\theta}} > 0 \tag{38b}$$

As done in the previous section, by replacing (38b) into the time derivative of (33), the asymptotic stability of this control system, that is $\tilde{\theta}(t) \to 0$ as $t \to \infty$, can easily be proved.

4.3. *Switching system*

These strategies imply switching between three behaviors: wall-following, orientation and rotation (circular path performer). The block diagram of the proposed switching control strategy is shown in Fig. 13. The switching signal σ generated by the supervisor, takes one of three possible values: a) $\sigma = 0$ if the controller for object-following is active, b) $\sigma = 1$ if the orientation controller is active and c) $\sigma = 2$ if the controller to perform a circular path is active.

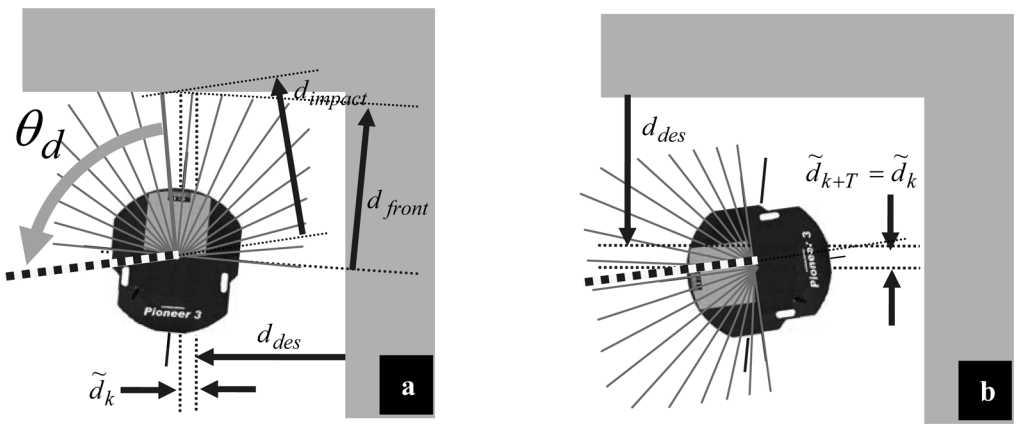

Fig. 11. Handling possible collision situations, (a) obstacle detected at instant k, and (b) free-path condition achieved with $\tilde{d}_{k+T} \leq \tilde{d}_k$ at instant (k+T).

https://doi.org/10.1017/S026357470800444X Published online by Cambridge University Press

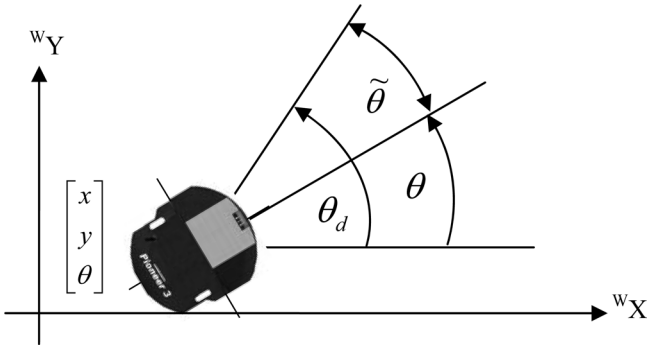

Fig. 12. Angular position controller description.

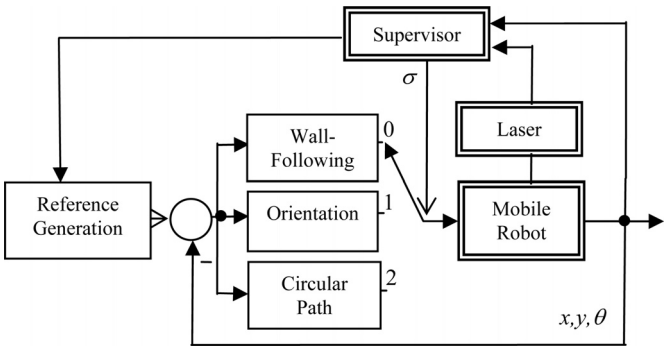

Fig. 13. Block diagram of the Contour-Following controller.

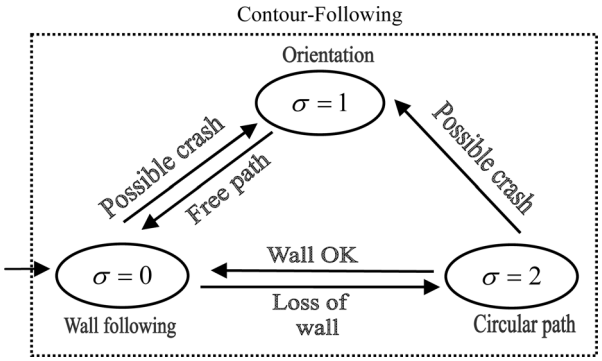

Fig. 14. Supervisor logic.

The transitions between these different behaviors can be summarized in the logic described in Fig. 14. The "Possible crash" condition is detected as an invasion of the guard-zone shown in Fig. 2(c) and the "Loss of wall" condition depends on the value of the variance computation over the length of the laser beams on the side of the robot.

4.4. Stability analysis

As is well known, it is possible to have unstable trajectories when switching among globally asymptotically stable systems.[26] Given a family of systems, it is desired that the switched system be stable for every switching signal σ. This is known as stability under arbitrarily switching[16] and has been the subject of several studies.[24–25] In fact, common Lyapunov functions are considered in order to prove stability for arbitrary switching, whereas multiple Lyapunov functions are used to prove stability for state-dependent switching (constrained switching). It is a know fact that finding a common Lyapunov function could be a difficult task, but if such function is found, the restrictions over the switching signal disappear, which allows for a stable switching between the involved controllers. So, a basic fact that is used in this section is that the existence of a common Lyapunov function with suitable properties guarantees uniform stability, as stated in Theorem I. A common Lyapunov function is defined as follows.

Given a continuously differentiable function $V : \Re^n \to \Re$; it is said to be a *common Lyapunov function* for the family of systems

$$\dot{\chi} = f_p(\chi) \quad p = 0, 1, 2, \ldots \tag{39}$$

if there exists a positive definite function $W : \Re^n \to \Re$ such that

$$\frac{\partial V}{\partial \chi} f_p(\chi) \leq -W(\chi) \quad \forall \chi, \ \forall p \in P. \tag{40}$$

Theorem I.[17] *If all the systems in the family (39) share a positive definite radially unbounded common Lyapunov function, then the switched system $\dot{\chi} = f_\sigma(\chi)$ is globally uniformly asymptotically stable (GUAS).*

The main point in this well-known theorem is that the rate of decrease of V along solutions, given by (39), is not affected by switching, hence asymptotic stability is uniform with respect to σ. Now, the purpose is to find a common Lyapunov function for the three continuous controllers. It is then first necessary to show that the closed-loop systems corresponding to each controller share a common equilibrium point at the origin. From Sections 3.3, 4.1 and 4.2, the closed-loop equations are

$$\dot{\chi} = f_0(\chi) = \begin{bmatrix} \dot{\tilde{\theta}} \\ \dot{\tilde{d}} \end{bmatrix} = \begin{bmatrix} -K_{\tilde{\theta}}(\tilde{\theta}) \tanh(k_{\tilde{\theta}}\tilde{\theta}) - k_{\tilde{d}}(\tilde{d})\,\tilde{d}\, v_{\max} \dfrac{\sin(\tilde{\theta})}{\tilde{\theta}} \\ -v_{\max} \sin(\tilde{\theta}) \end{bmatrix} \tag{41}$$

$$\dot{\chi} = f_1(\chi) = \begin{bmatrix} \dot{\tilde{\theta}} \\ \dot{\tilde{d}} \end{bmatrix} = \begin{bmatrix} -K_{\tilde{\theta}}(\tilde{\theta}) \tanh(k_{\tilde{\theta}}\,\tilde{\theta}) \\ 0 \end{bmatrix} \tag{42}$$

$$\dot{\chi} = f_2(\chi) = \begin{bmatrix} \dot{\tilde{\theta}} \\ \dot{\tilde{d}} \end{bmatrix} = \begin{bmatrix} -K_{\tilde{\theta}}(\tilde{\theta}) \tanh(k_{\tilde{\theta}}\,\tilde{\theta}) \\ 0 \end{bmatrix}. \tag{43}$$

It is clear that the origin is a common equilibrium point for the involved behaviors. Then, from (15) and (33), a common Lyapunov function for the switching among these controllers is given by (15). Therefore, it can be concluded that the switching control system composed by the three subsystems described in the previous sections is stable for any switching signal σ, because every behavior is at least stable considering the common Lyapunov function (15). However, the proposed application is composed by an asymptotically stable main behavior (wall-following) and two complementary stable

https://doi.org/10.1017/S026357470800444X Published online by Cambridge University Press

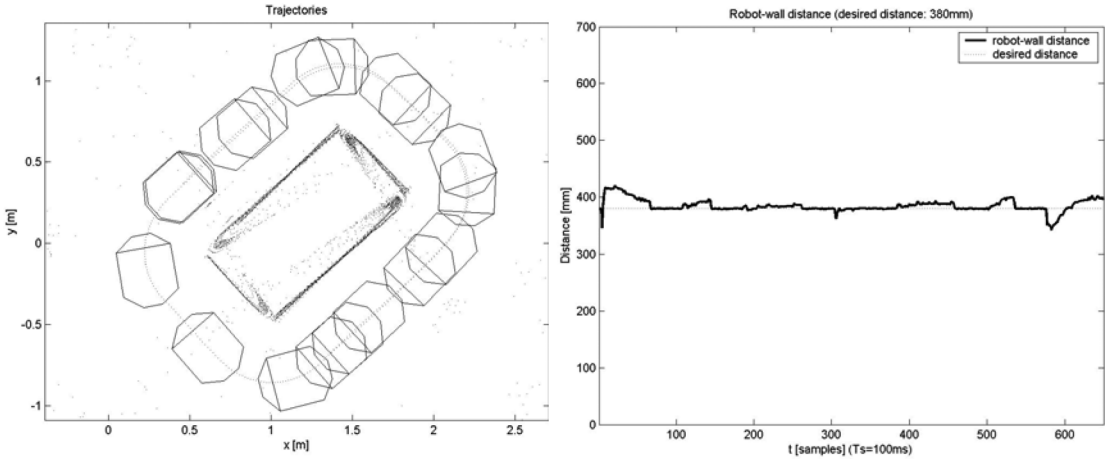

Fig. 15. Robot following a box contour.

behaviors (orientation and circular-path performer). As it was shown along this paper, the complementary behaviors are active only during special situations and the system always returns to the main behavior. Therefore, the GUAS property for the overall switched system an be concluded, provided that the wall following behavior is AS.

In summary, the continuous control actions that are being switched in this contour-following controller for $\sigma = 0$, $\sigma = 1$ and $\sigma = 2$ are, respectively,

$$v = v_{\max} \tag{44a}$$

$$\omega = \dot{\theta}_{\text{wall}} + K_{\tilde{\theta}} \tanh(k_{\tilde{\theta}}\tilde{\theta}) + k_{\tilde{d}}(\tilde{d})\,\tilde{d}\,v_{\max} \sin(\tilde{\theta})/\tilde{\theta} \tag{44b}$$

$$v = 0 \tag{45a}$$

$$\omega = K_{\tilde{\theta}} \tanh(k_{\tilde{\theta}}\,\tilde{\theta}) \tag{45b}$$

$$v = v_{\max} \tag{46a}$$

$$\omega = \theta_{\text{circ}} + K_{\tilde{\theta}} \tanh(k_{\tilde{\theta}}\tilde{\theta}) \tag{46b}$$

4.5. Experimental results

The switching contour-follower controller described in this paper has been implemented on a Pioneer III mobile robot navigating through a typical office environment at a linear speed of 150 mm/sec. The following figures show the trajectories described by the robot when following the interior contour of the building. As mentioned further above, the office contour was reconstructed by using the laser sensorial information. The controller constants were set to: $v_{\max} = 150$ mm/sec, $k_1 = 0.02$, $K_{\tilde{\theta}} = 0.25$ and $k_\theta = 5$. The sample time is 100 ms. The desired distance to the object was selected as 0.38 m, the selection of this value was based on the size of doors, and larger values for d_{wall} do not allow the robot to pass across them.

The first experiment (Fig. 15) shows a classic situation when following a non-smooth contour. The robot follows the outline of a rectangular box[3,5] at 380 cm. From this picture, and comparing it with other related papers,[3,5] the good performance of the proposed controller can be demonstrated.

In a second experiment, Fig. 16 shows the performance of the controller when switching between the wall-following controller and the re-orientation controller in an interior office setting.[3,5–6] In Fig. 17 a more complex setting shows the robot navigation along a usual corridor with an open door, which creates a trap situation[7] (or U-shaped obstacle) that is successfully avoided by the controller.

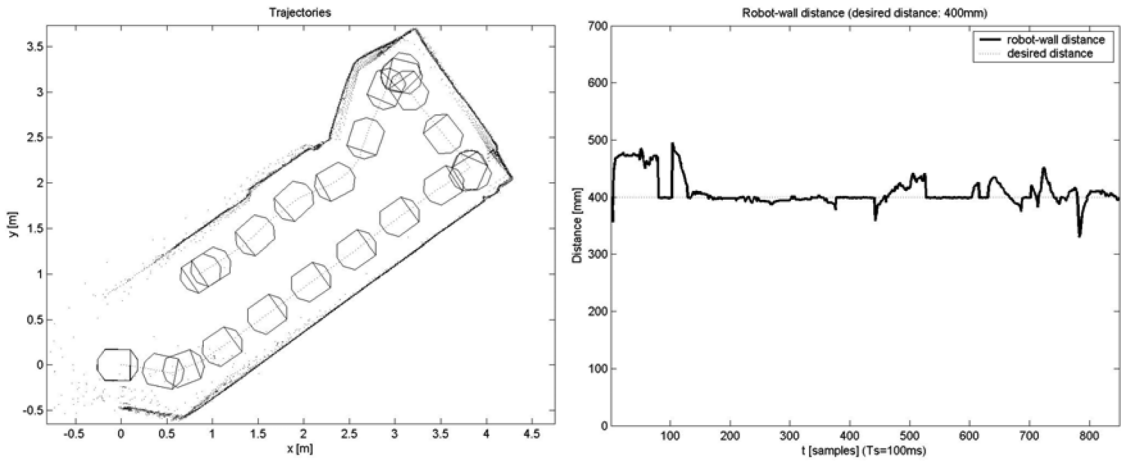

Fig. 16. Mobile robot following the interior contour of an office.

https://doi.org/10.1017/S026357470800444X Published online by Cambridge University Press

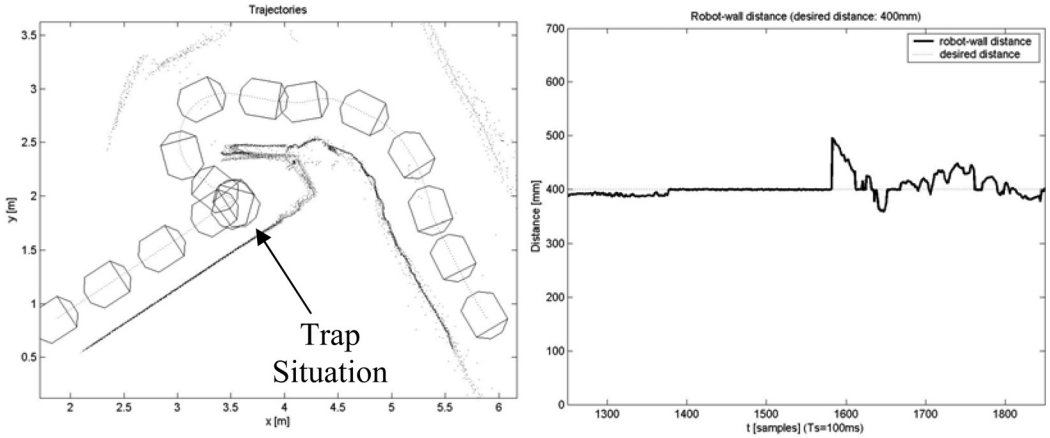

Fig. 17. Avoiding a trap situation generated by an opened door.

In the last experiments, the robot deals with unexpected obstacles,[2–3,7] including a block situation in the corridor. Figures 18 and 19 show the good performance of the controller when the robot avoids the obstacles. Figure 19 also shows a blocking situation in the corridor, which forces the robot to return along the opposite side of the corridor.

5. Conclusions

This paper has presented a wall-following controller that allows wheeled mobile robots to follow straight and smoothly varying walls contours at a desired distance. The works has also considered a switching controller that deals with the contour-following problem (following non-smooth contours.) In designing the control system, the asymptotic

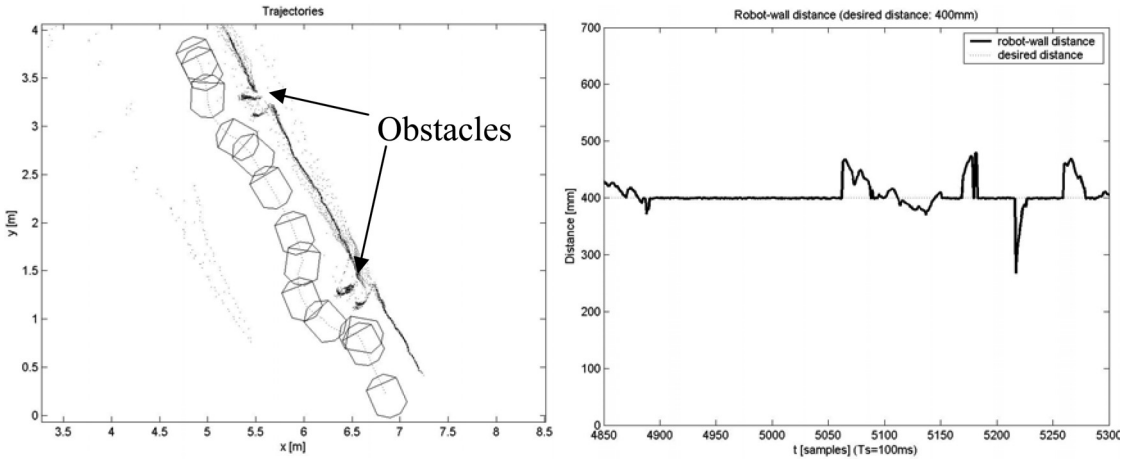

Fig. 18. Robot moving along a corridor avoiding obstacles.

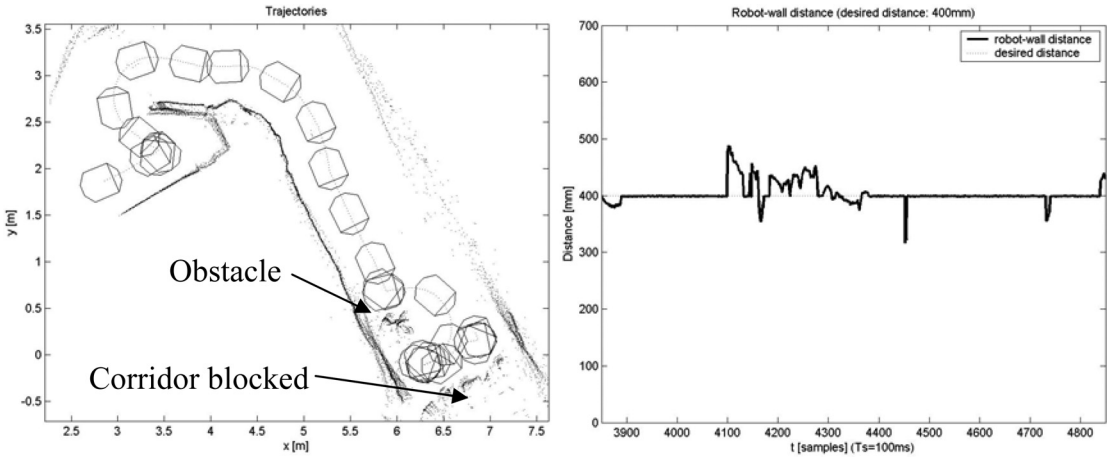

Fig. 19. Robot moving along a corridor avoiding obstacles and a block situation.

https://doi.org/10.1017/S026357470800444X Published online by Cambridge University Press

stability of the individual controllers as well the asymptotic stability at the switching times (for the switching controller) were considered and proved. Furthermore, the saturation of the control actions and the estimations of the control references were also regarded. Finally experimental results in a Pioneer III mobile robot with odometry and laser radar sensor have been included; showing the good performance of the proposed control strategy, when compared with other related works, in actual office environments. Future work will consider this controller as a sub-system in a more complete switching controller to perform complex autonomous tasks.

Acknowledgements

The authors gratefully acknowledge SETCIP and CONICET (Argentina) for partially funding this research.

References

1. R. C. Arkin, *Behavior-based Robotics* (MIT Press: Cambridge, MA, 1998).
2. M. J. L. Boada, F. J. Rodriguez, R. Barber and M. A. Salichs, "A Control System Based on Reactive Skills for Autonomous Mobile Robots," *IEEE International Conference on Advanced Robotics ICAR*, Coimbra, Portugal (2003).
3. R. Braunstingl and J. M. Ezkerra, "Fuzzy Logic Wall Following of a Mobile Robot based on the Concept of General Perception," *IEEE International Conference on Advanced Robotics ICAR*, Sant Feliu de Gíxols, Catalonia, Spain (1995) pp. 367–376.
4. M. Wang and J. Liu, "Autonomous Robot Navigation Using Fuzzy Logic Controller," *International Conference on Machine Learning and Cybernetics*, Shangai, China (2004) pp. 26–29.
5. Y. Ando and S. Yuta, "A reactive wall-following algorithm and its behaviors of an autonomous mobile robot with sonar ring," *J. Robot. Mech.* **8**(1), 33–39 (1996).
6. S. Fazli and L. Kleeman, "Simultaneous landmark classification, localization and map building for an advanced sonar ring," *Robotica* **25**, 283–296 (2007).
7. J. Borenstein and Y. Koren, "Real-time obstacle avoidance for fast mobile robots," *IEEE Trans. Syst. Man Cybern.* **19**(5), 1179–1187 (1989).
8. Z. Zhang, N. Sarkar and X. Yun, "Supervisory Control of a Mobile Robot for Agile Motion Coordination," *IEEE International Conference on Robotics and Automation ICRA*, Columbus, OH, USA (2004) pp. 2196–2203.
9. P. van Turennout and G. Hounderd, "Following a Wall with a Mobile Robot Using Ultrasonic Sensors," *Proceedings of the 1992 IEEE/RSJ International Conference on Intelligent Robots and Systems*, Raleigh, NC, USA (1992) vol 2, pp. 1451–1456.
10. E. Bicho, "Detecting, Representing and Following Walls based on Low-level Distance Sensors," *Proceedings of the 2nd International Symposium on Neural Computation*, Berlin, Germany (2000).
11. T. Edlinger and E. von Puttkamer, "Exploration of an Indoor-Environment by an Autonomous Mobile Robot," *IEEE International Conference on Intelligent Robots and Systems IROS* (2004) vol 2, pp. 1278–1284.
12. R. Brawn and P. Hwang, *Introduction to Random Signals and Applied Kalman Filtering*, 3rd ed. (John Wiley & Sons, New York, 1997) pp. 371–375.
13. J. M. Toibero, R. Carelli and B. Kuchen, "Wall-Following Stable Control for Wheeled Mobile Robots," *International IFAC 8th Symposium on Robot Control SYROCO*, Bologna, Italy (2006b).
14. R. Kelly and R. Carelli, "A class of nonlinear PD-type for robot manipulator," *J. Robot. Syst.* **13**(12), 793–802 (1996).
15. J. M. Toibero, R. Carelli and B. Kuchen, "A Stable Switched Contour-following Controller for Wheeled Mobile Robots," *IEEE International Conference on Robotics and Automation ICRA*, Orlando, FL, USA (2006a).
16. D. Liberzon, *Switching in Systems and Control* (Birkhauser, Boston, 2003).
17. M. Branicky, "Multiple Lyapunov Functions and other analysis tools for switched and hybrid systems," *IEEE Trans. Autom. Control* **43**(4), 475–482 (2004).
18. J. M. Toibero, R. Carelli and B. Kuchen, "Switching Control of Mobile Robots for Autonomous Navigation in Unknown Environments," *IEEE International Conference on Robotics and Automation ICRA*, Roma, Italy (2007) pp. 1974–1979.
19. S. Jung, P. Jeon and T. C. Hsia, "Contour tracking of an unknown planar object by regulating force for mobile robot navigation," *Robotica* **25**, 297–305 (2007).
20. H. R. Everett, G. A. Gilbreath, T. A. Heath-Pastore and R. T. Laird, "Controlling Multiple Security Robots in a Warehouse Environment," *AIAA-NASA Conference on Intelligent Robots, Houston*, Houston, TX, USA (1994) pp. 93–102.
21. S. Garrido, L. Moreno, D. Blanco and M. L. Munoz, "Sensor-based global planning for mobile robot navigation," *Robotica* **25**, 189–199 (2007).
22. R. C. Arkin, "Reactive control as a substrate for telerobotic system," *IEEE AES Syst. Mag*. 24–31 (1991).
23. M. Vidyasagar, *Nonlinear Systems Analysis*, 2nd ed. (Prentice-Hall, Englewood Cliffs, NJ, 1993).
24. L. Vu and D. Liberzon, "Common Lyapunov Functions for families of commuting nonlinear systems," *Syst. Control Lett*. **54**, 405–416 (2005).
25. J. L. Mancilla-Aguilar, "A condition for stability of switched nonlinear systems," *IEEE Trans. Autom. Control* **45**(11), 2077–2079 (2000).
26. D. Liberzon and A. S. Morse, "Basic problems in stability and design of switched systems," *IEEE Control Syst. Mag*. **19**(5), 57–70 (1999).

https://doi.org/10.1017/S026357470800444X Published online by Cambridge University Press